Electronic Supplementary Material

Ultrasonic-shear exfoliated multi-layer graphene flakes for enhanced triboelectric nanogenerator performance toward wearable self-powered applications

Honghao Zhang[a], lele Gao[b], Hua Huang[a], You lv[a], Baocheng Liu[c], Ping Zhang[c], Robert Tomala[d], Zhengchun Yang[e*] and Le Zhang[a*]

[a] *Jiangsu Key Laboratory of Advanced Laser Materials and Devices, School of Physics and Electronics Engineering, Jiangsu Normal University, Xuzhou, 221116, P.R. China*
[b] *Rare Earth Advanced Materials Technology Innovation Center，Inner Mongolia Northern Rare Earth Advanced Materials Technology Innovation Co., Ltd.，Baotou 014030, P.R.China*
[c] *School of Electrical and Information Engineering, Tianjin University, Tianjin 300072, P. R. China.*
[d] *Institute of Low Temperature and Structure Research, Polish Academy of Sciences, 50-422 Wroclaw, Poland.*
[e] *School of Integrated Circuit Science and Engineering, Advanced Materials and Printed Electronics Center, Tianjin Key Laboratory of Film Electronic & Communication Devices, Tianjin University of Technology, Tianjin 300384, China*
**Corresponding author.*
Email address: yangzhengchuntjut@163.com(Zhengchun Yang)
zhangle@jsnu.edu.cn (Le Zhang)

1 Supporting Figures

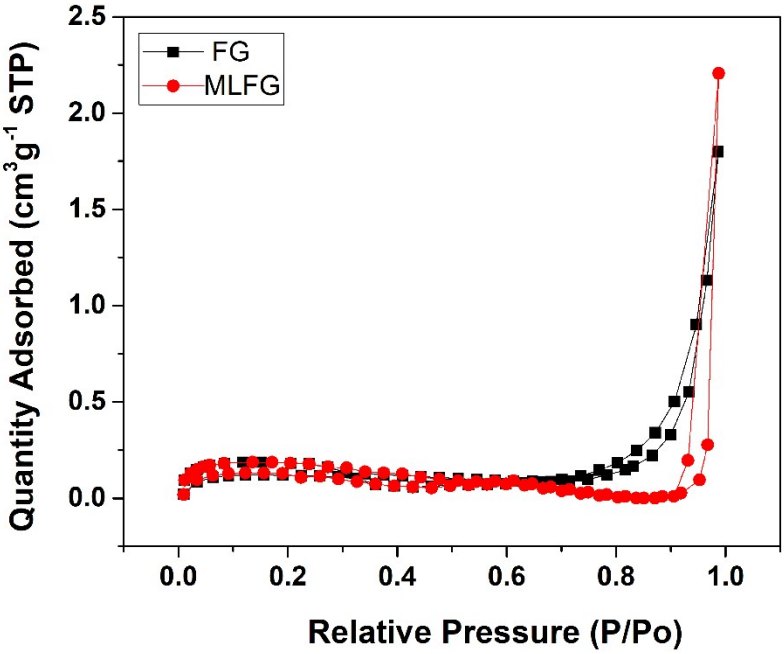

Fig. S1. BET test of FG and MLFG.

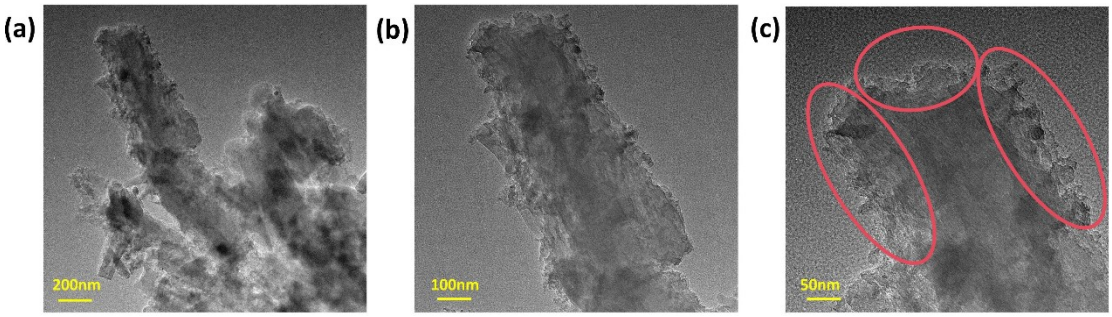

Fig. S2. TEM image of MLFG.

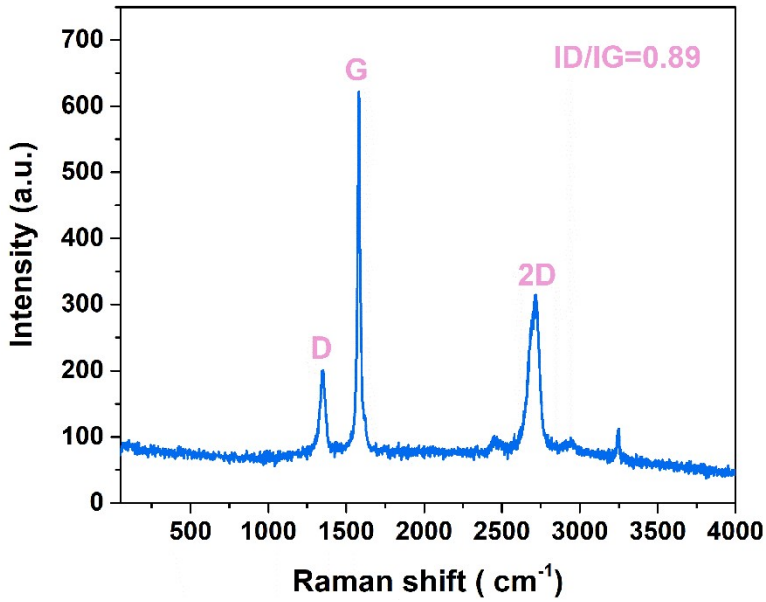

Fig. S3. Raman spectrum of MLFG.

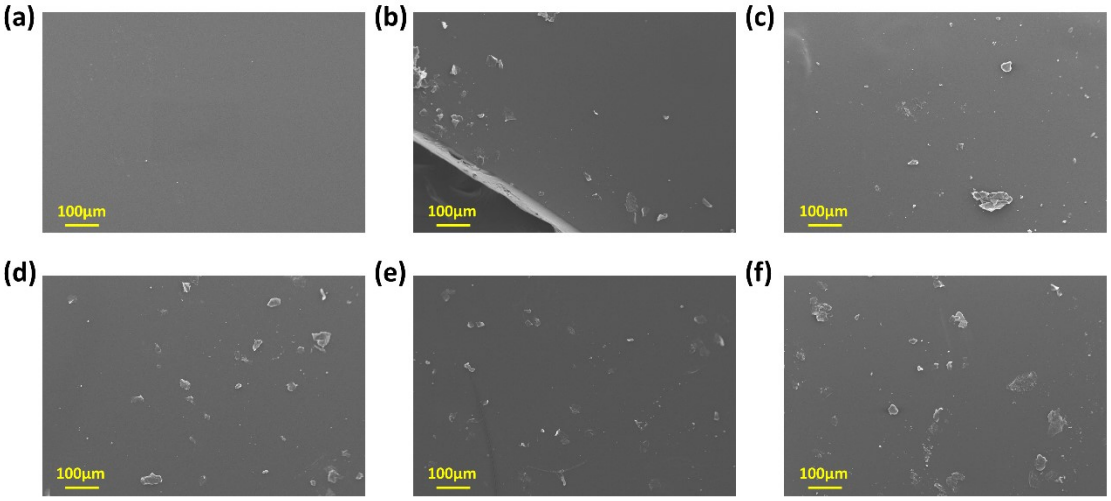

Fig. S4 Morphology of PDMS@FG with Different Doping Weight Ratios. (a) 0wt% FG; (b) 1wt% FG; (a) 2wt% FG; (b) 3wt% FG;(a) 4wt% FG; (b) 5wt% FG.

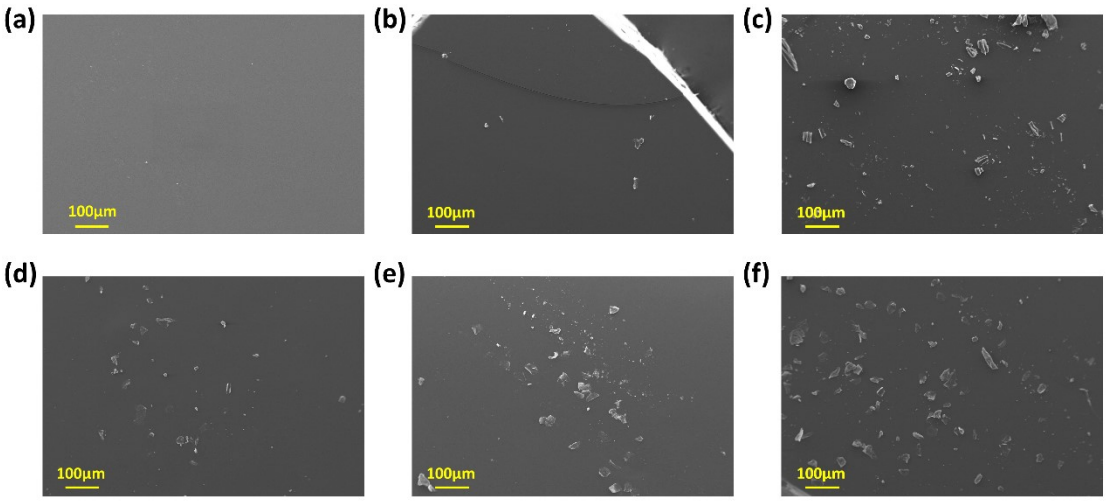

Fig. S5 Morphology of PDMS@MLFG with Different Doping Weight Ratios. (a) 0wt% MLFG; (b) 1wt% MLFG; (a) 2wt% MLFG; (b) 3wt% MLFG;(a) 4wt% MLFG; (b) 5wt% MLFG.

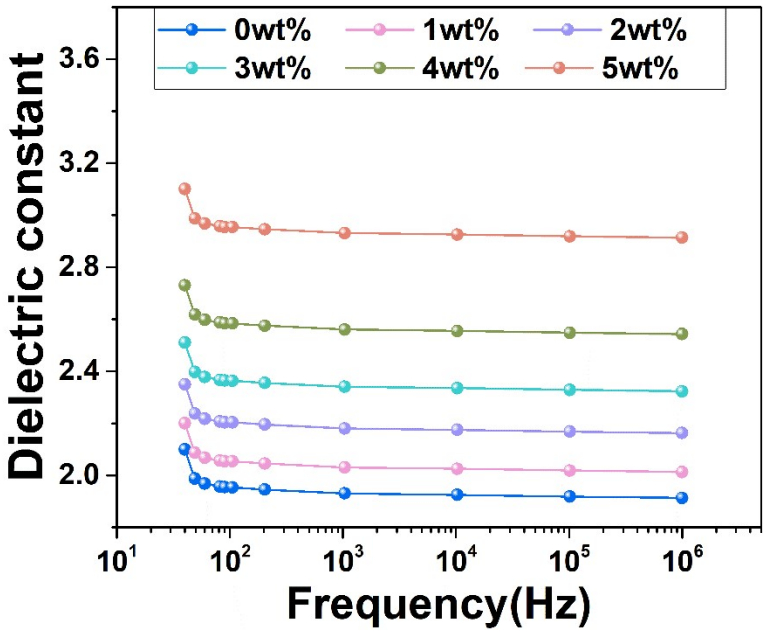

Fig. S6. Dielectric properties of MLFG.

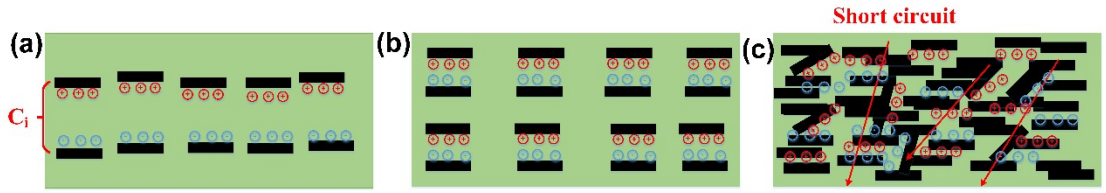

Fig.S7. (a-c) Schematic diagram of the PDMS@MLFG film's microstructure change with different weight ratios of MLFG.

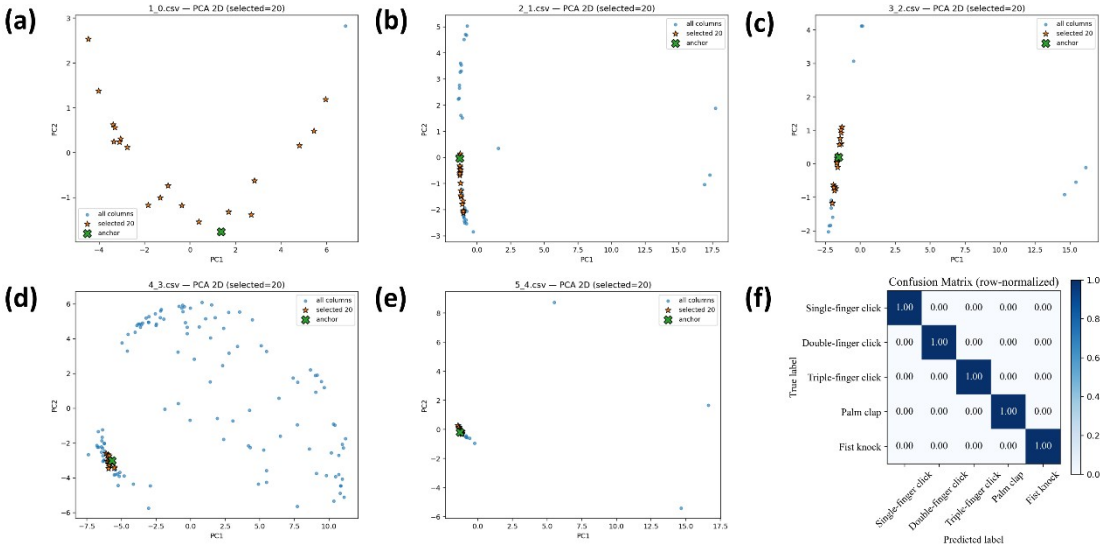

Fig.S8. PCA Distribution and Classification Results for Gesture Datasets. (a–e) Two-dimensional PCA projections of five gesture datasets: single-finger click, double-finger click, triple-finger click, palm clap, and fist knock. Blue dots represent all feature vectors, orange asterisks denote the 20 selected key features, and green crosses indicate anchor samples; (f) Row-normalized confusion matrix of the gesture recognition model across the five gesture categories.

In this study, the dataset comprises 150 continuous gesture samples, covering five types of gestures. Each gesture was repeated more than 30 times along the same trajectory. To process the continuous data, a data segmentation method was employed to divide each gesture into multiple independent samples. To avoid generating a large number of highly similar redundant samples after segmentation, an unsupervised similarity clustering approach was applied to analyze the segmented gesture fragments. This allowed the selection of 20 representative samples per gesture category without introducing any class-discriminative information, resulting in a total of 100 samples for subsequent modeling. This process was solely used for sample deduplication and representative selection and did not involve any model training or classification information. During dataset construction, four samples were randomly selected from each gesture category to form an independent test set, while the remaining samples were used for model training. Finally, the dataset was split into training and test sets in an 80% : 20% ratio, with the test set kept entirely separate throughout model training to evaluate the recognition performance on unseen samples. All experiments were repeated multiple times to ensure the stability and reliability of the results.

Table S1. Fabrication and Performance Comparison of MLFG and Similar Carbon Materials as TENG Triboelectric Layers

Material	Output (V)	Power Density ($\mu W\ cm^{-2}$)	Fabrication Process	Cost	Ref.

Chitosan/Activated Carbon/PTFE	75.44	2.7	Hydrolysis Reaction (Complex)	High	**1**
Milk-Derived Porous Carbon/PTFE	20 V	5.6	Tube Furnace Calcination (Complex)	High	**2**
Ecoflex/Porous Carbon/PDMS	115.9	11.6	Spin Coating (simple)	Low	**3**
rGO/PRTNF	228.26	28.67	Hydrothermal Reduction (Complex)	High	**4**
PI/PTFE	430	138	Laser-Induced Graphene (Complex)	High	**5**
SC-rGO/PTFE	81.5	255	Thermal Annealing (Complex)	High	**6**
PDMS/MLFG/Polyester	90.3	20.9	Ultrasonic-Shear Exfoliation (simple)	Low	**This Work**

References

1. E. Chaturvedi and P. Roy, *Acs Applied Energy Materials*, 2024, **7**, 9735-9745.
2. X. Hou, P. G. Ren, Z. Z. Guo, W. H. Tian, Y. L. Wang, B. L. Fan, H. T. Chen, Z. Y. Chen and Y. L. Jin, *Journal of Power Sources*, 2025, **649**.
3. J. Zhao, Y. Xiao, W. Yang, S. C. Zhang, H. N. Wang, Q. Wang, Z. Y. Sun, W. J. Li, M. Gao, Z. F. Wang, Y. Xu, H. M. Chen and J. Wang, *Advanced Materials Technologies*, 2023, **8**.
4. F. L. Shi, X. Wei and X. Q. Wu, *Chemical Engineering Journal*, 2024, **494**.
5. W. X. Yang, M. G. Han, F. Liu, D. Wang, Y. Gao, G. T. Wang, X. L. Ding and S. D. Luo,

Advanced Science, 2024, **11**.

6. H. J. Hwang, J. S. Yeon, Y. Jung, H. S. Park and D. Choi, *Small*, 2021, **17**.